Parametric Sensitivity Study of a CFD-Based Coal Combustion Model

Joseph D. Smith, Philip J. Smith, and Scott C. Hill
Dept. of Chemical Engineering, University of Utah, Salt Lake City, UT 84112

Parametric sensitivity of a two-dimensional pulverized-fuel (PF) combustion model is studied extensively for the effect of parametric uncertainty on model predictions. Results show that error in coal devolatilization/oxidation parameters has the dominant effect on predicted burnout, NO_x formation, local gas temperature, and coal-gas mixture fraction. Uncertainty in the turbulent particle dispersion parameters appears to have a secondary effect, while error in the particle-gas radiation parameters has little impact on model predictions. Regions of the computational domain exhibiting sensitivity to specific parameters are identified. Specific parameter sensitivity implies the relative importance of various mechanisms in the overall process. Turbulent particle dispersion seems to be important early in the reactor with kinetic processes dominating at and following the predicted ignition point. Radiation appears to be of minor importance. These results indicate the need for a better method of predicting the overall volatiles yield and further understanding of the devolatilization/oxidation mechanism and its role in the overall PF combustion process. The study provides fundamental direction for future comprehensive model development and focuses on experimental work to better quantify critical input parameters.

Introduction

Sensitivity analysis has its early roots in stability analysis of ordinary differential equations related to classical mechanics (Tomovic and Vokobratovic, 1972). More recently, sensitivity analysis has been associated with error analysis (Frank, 1978). One of the greatest benefits of a sensitivity analysis is the physical understanding of a complex process gained by performing the analysis.

The general sensitivity problem can be stated as:

$$Lu(x, \alpha) = S \tag{1}$$

L represents the general mathematical operator, $u = (u_1, u_2, u_3, ., ., .u_n)$ represents the vector of model outputs which are determined by the independent variables $x = (x_1, x_2, x_3, ., ., .x_n)$ and the model parameters $\alpha = (\alpha_1, \alpha_2, \alpha_3, ., ., .\alpha_n)$. $S = (S_1, S_2, S_3, ., ., .S_n)$ represents the source terms or forcing functions corresponding to the respective equations in the set. All parameters represented by α have some degree of uncertainty over a range:

$$\alpha_i^- < \alpha_i^0 < \alpha_i^+, \; i = 1, 2, 3, ., ., ., \text{number of parameters} \tag{2}$$

which can be represented by some probability density function (PDF), $f(\alpha_i)$, such that the probability (P) that α_i is between α_i^- and α_i^+ is:

$$P(\alpha_i^0) = \int_{\alpha_i^-}^{\alpha_i^+} f(\alpha_i) d\alpha_i \tag{3}$$

For completely independent parameters, the probability functions for each parameter can be combined to form a joint PDF representing the most probable parameter space:

$$f(\alpha) = \prod_{i=1}^{n} f_i(\alpha_i) \tag{4}$$

Correspondence concerning this article should be addressed to J. D. Smith at Dow Chemical Company, Midland, MI 48667.
Current address of S. C. Hill: 75 CTB, Brigham Young University, Provo, UT 84602.

The main goal of a sensitivity analysis is to simultaneously vary all parameters over all probable combinations (representing parameter uncertainty) and to quantify the effects this variation has on a specified model output. Better estimates of the key parameters representing less parametric uncertainty can then be used to obtain more realistic model predictions.

During the initial developmental stages of a numerical model of a particular system one must invariably test the model for a finite number of parameter values which characterize the system. This represents a crude form of sensitivity analysis and would represent a global sensitivity analysis if the model were tested at all possible parameter values. Of course, this type of analysis is not feasible for realistic problems, so various types of sensitivity analysis techniques have been developed to approximately examine the total parameter space. These techniques include one-at-a-time ("brute force") methods, local (finite differences, direct differential and adjoint "Green's function" methods, and global nonlinear (FAST and stochastic) methods.

One-at-a-time methods are commonly referred to as trend analysis. This entails holding all parameters but one constant and observing the effects variations in one parameter have on a specific model prediction. This technique does not provide complete coverage of the probable parameter space. Linear methods require one to vary parameters between a high and a low value to approximate the sensitivity coefficient ($du_i/d\alpha_j$) for the ith output function with respect to the jth parameter. This method is limited to small parameter ranges because of the linear difference approximation to the sensitivity coefficient. In most cases, this approximation can only account for the direct effects (u_i is a function of α_j) of a parameter on a function. This neglects the possibility that a parameter, not in the function, may have an indirect but significant effect on the prediction. Finally, global nonlinear methods provide the most detailed sensitivity information. These methods can be applied over all probable parameter values and account for both direct and indirect parameter effects. This last feature allows one to investigate the sensitivity of model predictions to simultaneous variations in two or more parameters. Each method has its place and can provide information about model sensitivity to parametric uncertainty.

Early global sensitivity techniques required great computational expense. However, recent development of efficient global methods have made it more feasible to conduct comprehensive sensitivity analysis of complex models, such as PCGC-2. Efficient techniques, described in the literature, include direct methods (Atherton et al., 1975; Dickinson and Gilinas, 1976; Caracotsios and Stewart, 1985; Dunker, 1981), orthogonal polynomial methods (Cukier et al., 1978; Pierce and Cukier, 1981) and methods based on Green's function (Hwang et al., 1978; Dougherty, 1979; Kramer et al., 1981; Rabitz et al., 1983). Each of the techniques reviewed have been used to study various physical systems. The focus of most sensitivity work has been on examining mechanistic chemical kinetic systems (Cukier et al., 1973; Boni and Penner, 1977; Pierce and Cukier, 1981; Hwang et al., 1978; Hwang, 1983; Smooke et al., 1986; Rabitz, 1981). Other work has focused on reaction-diffusion systems (Coffee and Heimerl, 1983; Reuven et al., 1986) and on simple pf combustion systems (Smith, 1984). The work described herein concerns a sensitivity study of a comprehensive model describing a pf combustion system.

Full-Scale Sensitivity Study of Complex Models

The equation set describing pf combustion in PCGC-2 is composed of several coupled nonlinear elliptic partial differential equations:

$$\frac{\partial}{\partial x}(\bar{\rho}\tilde{u}\tilde{\phi})+\frac{1}{r}\frac{\partial}{\partial r}(r\bar{\rho}\tilde{v}\tilde{\phi})-\frac{\partial}{\partial x}\left(\Gamma_\phi\frac{\partial\tilde{\phi}}{\partial x}\right)-\frac{1}{r}\frac{\partial}{\partial r}\left(r\Gamma_\phi\frac{\partial\tilde{\phi}}{\partial r}\right)=\overline{S_\phi} \quad (5)$$

Given the appropriate boundary conditions and source terms, it is possible to describe, in the Eulerian sense, the conservation of turbulent mass, momentum and energy transport in both the gas- and the particle-phases with the general convection-diffusion equation shown in Eq. 5. A detailed description of PCGC-2 is not included here but is well documented elsewhere (Smith et al., 1981; Smoot and Smith, 1985). Due to the complexity of the model, a converged solution requires substantial computational effort (approximately 15 CPU hours on a VAX 11/750). To describe the complex mechanisms occurring in pf combustion a large number of physical parameters are required. The relationship between model predictions (that is, coal burnout, NO_x concentration, local gas temperature, and so on) and parameters (that is, kinetic rate constants, turbulence parameters, radiation parameters, and so on) uncertainty is nonlinear. These constraints limit the number of parameters that can be examined and the type of sensitivity method that can be used.

To make the sensitivity study comprehensive, the methodology must be able to include a reasonable number of model parameters (representing the several mechanisms of pf combustion) and be capable of analyzing a nonlinear response surface while requiring a feasible amount of computational effort. None of the techniques reviewed in a literature survey met these criteria for reasons discussed earlier. Therefore, a unique methodology was developed that is particularly useful for studying large, complex computer codes requiring substantial computational time. This method was established by combining two techniques previously developed for different applications. The resulting methodology proceeds in two steps. The first step employs a linear sensitivity technique or screening design to screen the initial parameter set for those parameters with primary effects.The second step incorporates a global nonlinear sensitivity technique which examines only those parameters identified in step one. The procedure used during each step of the study will be discussed in the following section.

Screening design

Screening designs, or fractional factorial designs, are obtained by performing a fraction of a total factorial design. In the absence of experimental variability, a completely saturated fractional factorial design is capable of screening out real parameter effects. A completely saturated design consists of $n+1$ simulations for n parameters. These techniques are commonly employed in quality control of manufacturing processes. A screening design is based on the assumptions that functional response is well behaved with some curvature but no kinks or inflection points in the response surface, and that effects of

Table 1. Input Parameters for the Screen Design

Parameter Name*	Description	Range	Researchers
VISCOS (kg/ms)	Approximate laminar viscosity for entire reaction chamber	$3.90-552\ (10^{-5})$	
PRK	Turbulent Prandtl/Schmidt number for particle dispersion	0.30 – 1.00	Smith et al. (1981); Fletcher (1983)
GAMMA	Particle swelling parameter	0.00 – 0.20	Smoot and Pratt (1979)
XI	Particle surface area factor	1.00 – 2.00	Smoot and Smith (1985)
EMJ(1,1) (J/kmol)	Activation energy for first devolatilization reaction	$7.36-10.46\ (10^{7})$	Smoot and Smith (1985)
EMJ(1,2) (J/kmol)	Activation energy for second devolatilization reaction	$16.73-10.46\ (10^{7})$	Smoot and Smith (1985)
YY(1,1)	Stoichiometric coefficient for first devolatilization reaction	0.30 – 0.39	Smoot and Smith (1985)
YY(1,2)	Stoichiometric coefficient for second devolatilization reaction	0.80 – 1.00	Smoot and Smith (1985)
EL(1,1) (J/kmol)	Activation energy for char oxidation energy	$8.35-9.30\ (10^{7})$	Smith et al. (1981); Smoot and Smith (1985)
WIC(1,3)	Elemental mass fraction of hydrogen in coal particles	0.049-0.054	Singer (1981)
WIC(1,4)	Element mass fraction of oxygen in coal particles	0.159 – 0.205	Singer (1981)
WIC(1,5)	Elemental mass fraction of nitrogen in coal particles	0.013 – 0.016	Singer (1981)
PHIL	Stoichiometric coefficient for oxidizer in char reaction	1.00 – 2.00	Smith et al. (1981)
QAB	Absorption efficiency for radiation from particles	0.80 – 1.00	Smoot and Pratt (1979)
QSC	Scattering efficiency for radiation from particles	0.20 – 0.50	Smoot and Pratt (1979)
EMW	Reactor wall emittance	0.50 – 0.90	Smith (1984)
URF**	Gas velocity under relaxation numerical parameter	0.45 – 0.55	
TINFLO	Turbulence intensity in the primary inlet stream	0.135 – 0.165	Smith et al. (1981); Smoot and Smith (1985)
TINFLO(2)	Turbulence intensity in the secondary inlet stream	0.162 – 0.180	Smoot and Smith (1985)

*FORTRAN variable names from PCGC-2.
**All gas velocity under-relaxation factors were changed together as one parameter.

one factor can depend on the level of one or more of the other factors.

The present study employed a "Plackett-Burman" design which is available in multiples of 4 from 4 to 100 runs. A saturated design for the 19 parameters shown in Table 1 required 20 converged PCGC-2 simulations. The main objective of this step was to identify those parameters exhibiting significant primary effects. Higher order effects are not addressed during the screening design but are examined thoroughly in the final phase of the sensitivity study.

The parameters shown in Table 1 consist mainly of physical parameters describing the combustion process (radiation, turbulent fluid mechanics, devolatilization, and so on). One numerical parameter, thought to have a significant effect on model predictions, was also included. Parameter ranges were established from a literature search or from experts in the field. Special effort was made to select parameters completely independent from one another to avoid confounding (masking important effects by combinations of parameters dependent upon each other) during the screening design. To characterize the uncertainty in the parameters between their low and high extremes some assumption about their probability density function was required. In the absence of any information concerning the error function, a normal distribution is usually selected to represent the randomness of the data. In the present study, the parameter ranges were identified from the literature or expert experience. These ranges represented reasonably probable values for the specific parameters. For a normal distribution, the ranges indicated in Table 1 would represent a three-standard-deviation confidence interval (99% confident of observed value being in range). In this study, no one value was assumed to be more probable than another in the range resulting in the selection of a uniform error function. This assumption was not necessary for the screening design but was important in the second phase of the study and is discussed later. A base case, well characterized by experimental work, was identified to provide a mean input data set based on the parameters shown in Table 1. Again, only the two extremes were used in the screening design and the mean value was not used, but was necessary for the second phase of the study. A summary of model input describing the reactor geometry and the operating conditions for the base case is presented in Table 2.

To characterize parameter effects as significant, it was necessary to select several predicted values from the model. A plethora of outputs characterizing the specific case are provided by PCGC-2 and it is not feasible to utilize all the information in a meaningful manner. Therefore, it was necessary to select a subset of the possible outputs that best quantified parameter effects. Seven such output values as shown in Table 3 were identified. Care was taken to select outputs that represent the main characteristics (that is, turbulent mixing and fluid mechanics processes, homogeneous and heterogeneous reaction processes, mass and energy transport processes, and so on) of pf combustion.

To complete the screening design for the initial parameter set, input for 20 separate cases was prepared by setting the parameters to their low or high value of the ranges shown in Table 1 according to the design pattern. Each case was converged and values for the output functions shown in Table 3 were recorded. These values were analyzed to determine parameter effects. Effects were classified as significant by a two-

Table 2. Summary of Base Case Data Describing Reactor Geometry and Operating Conditions

Geometry		*Feed Rates*	
Primary tube diameter (m)	0.022	Primary gas (kg/s)	6.228 (10^{-3})
Secondary tube diameter (m)	0.084	Secondary gas (kg/s)	0.019
Chamber diameter (m)	0.203	Coal in Primary (kg/s)	2.835 (10^{-3})
Chamber length (m)	1.561		
Inlet Gas Properties		*Reactor Parameters*	
Primary swirl number	0.000	Reactor Pressure ($N/m^2 \cdot m$)	8.60 (10^4)
Primary turbulence intensity (%)	15.0	Side wall Temperature (K)	1,000.00
Primary temperature (K)	300.0		
Primary mole fractions:		*Particle Parameters*	
AR	0.046	Particle solid density (kg/m^3)	1,340.0
H_2O	0.035	High Heating Value, dmmf (J/kg)	2.97 (10^7)
N_2	0.725		Mass mean
O_2	0.194		
Particle diameter (m)	5.025 (10^{-5})	Initial analysis:	
Secondary swirl	2.000	raw coal	0.931
Secondary turbulent intensity (%)	18.0	ash	0.069
Secondary temperature (K)	589.0	Elemental analysis (daf):	
Secondary mole fractions:		C	0.752
AR	0.009	H	0.051
N_2	0.781	O	0.182
O_2	0.210	N	0.015

sided t-test with an 80% confidence interval and 19 degrees of freedom. Each output function produced a different subset of key parameters. A list of the most crucial parameters was formed by combining the results from each output function. Table 4 shows the final set of nine (from the original 19) parameters chosen for further study. The first six parameters shown in Table 4 had a t-statistic greater than the critical t-statistic (significant effect) indicating a primary effect. The last three parameters had t-statistics less than but very near the critical t-value and were included to examine the possible nonlinear effects caused by high-order coupling. Together, these nine parameters formed the final set for examination in the global sensitivity analysis.

Results from the screening design indicate that uncertainty in devolatilization and turbulent particle dispersion parameters have a dominant impact on model predictions, as indicated by comparing the corresponding t-statistic to the critical value. Uncertainty in the radiation coefficient, char oxidation parameters and gas-turbulence parameters had a less significant (again based on small t-statistics) effect on model predictions.

Global sensitivity analysis

After reviewing various techniques capable of performing a global sensitivity analysis of PCGC-2, FAST was selected for the final step of the sensitivity study. This selection was based upon prior experience with the technique and the availability of a computer code to perform the analysis (Pierce, 1981). In addition, FAST is a well proven technique that has been used in several engineering disciplines to aid in validation of math-

Table 3. Screening Design Output Functions and Results

Output Function	Comments	Significant Parameters*	*t*-statistic**
Carbon conversion at reactor exit (%)	Reflects overall combustion characteristics	EMJ(1,2),	−3.36
		PHIL(1)	1.39
Maximum axial centerline gas temperature (K)	Represents degree of mixing and combustion	PRK,	−1.54
		GAMMA,	−1.34
		EMJ(1,2)	−2.97
Maximum axial flame front gas temperature	Reflects devolatilization/ oxidation and flame structure characteristics	EMJ(1,2)	2.15
Flame front axial position in reactor (cm)	Reflects flame structure characteristics	EMJ(1,2),	3.53
		PHIL(1)	−1.36
Carbon conversion at flame front (%)	Relationship between particle reactions and gas temperature	PRK,	1.23
		EMJ(1,2)	−3.15
Percent of total carbon conversion at flame front (%)	Relationship between particle reactions and total carbon conversion	PRK,	−2.26
		EMJ(1,2)	−2.56
		WIC(1,4)	1.45
Mixing cup NO_x concentration at reactor exit (ppm)	Reflects pollutant formation characteristics	PRK,	−1.59
		EMJ(1,2),	2.83
		QSC	−1.56

*FORTRAN variable names from PCGC-2.
**Critical *t*-statistic for two-sided *t*-test with eighteen DOF is 1.33.

Table 4. Parameters Examined in Step Two of the Sensitivity Study

Parameter	Units	Base Value	Uncertainty
Turbulent Particle Schmidt Number	--	0.65	0.35
Particle Swelling Factor	--	0.10	0.10
Activation Energy for High Temperature Devolatilization Reaction	(10^7) J/kmol	20.90	4.20
Stoichiometric Coefficient for High Temperature Devolatilization Reaction	--	0.90	0.10
Activation Energy for Char Oxidation Reaction	(10^7) J/kmol	8.80	0.40
Elementary Mass Fraction of Oxygen in Particle	--	0.18	0.02
Stoichiometric Coefficient for the Oxidizer in the Char Oxidation Reaction	--	1.50	0.50
Turbulence Intensity of Primary Gas Stream	--	0.15	0.05
Scattering Efficiency for Particle Radiation	--	0.35	0.15

ematical models (Boni and Penner, 1977; Pierce, 1981; Pierce and Cukier, 1981; Smith, 1984; Kuntz et al., 1976; Koda et al., 1979; Falls et al., 1979; Tilden et al., 1981). Only a brief review of the salient features of the method are given here, but a detailed description of the theoretical development of the techniques is given elsewhere (Cukier et al., 1978).

FAST statistically varies all parameters simultaneously over the probable parameter space in a sinusoidal fashion with a specific frequency assigned to each parameter. This method was shown to provide a good approximation to the probable parameter space (Pierce, 1981). Results from model predictions, corresponding to unique parameter sets, are Fourier-analyzed. The number of unique parameter sets, which corresponds to the number of computer simulations (N), required to obtain the sensitivity information for n parameters is approximated as:

$$N \approx n^{2.5} \tag{6}$$

More specifically, the total number of simulations required in a FAST sensitivity analysis is determined by the maximum sampling frequency. This frequency is based on the Shannon Sampling Theorem (Jerri, 1965) and the order of accuracy of the frequency set (Schailby and Schuler, 1973).

The Fourier coefficients are used to determine variables that quantify sensitivity of the predictions to input uncertainty. The average prediction, total deviation of the average prediction and the individual contribution to the total deviation caused by uncertainty in each parameter are calculated. Using these sensitivity variables, the parameter uncertainty causing the greatest variance in model predictions can be determined.

There are two main errors inherent in the FAST technique: aliasing and biasing. Aliasing errors occur when the frequencies oscillate at a greater rate than the functional sampling rate. Cukier (1975) showed that it is necessary to conduct a number of simulations equal to at least twice the maximum frequency to minimize the aliasing error. The maximum frequency of the frequency set is determined by the degree to which the set approximates an incommensurate set. Biasing is caused when two or more of the frequencies of the set combine to form another set frequency. Cukier (1975) describes methods used to obtain frequency sets free of baising to different levels of accuracy. The more accurate the frequency set, the larger the maximum frequency and the larger the corresponding increase in the required number of model simulations. An in-depth study of these two errors in the global sensitivity analysis of PCGC-2 was conducted in an earlier study (Smith and Smoot, 1987) to validate the sensitivity results.

The sensitivity analysis of PCGC-2 required a large amount of computer time even with a small subset of the original list of input parameters. To accomplish this portion of the study in a reasonable amount of time, the computer calculations were performed on the Cray computers at Los Alamos National Laboratory in New Mexico. The sensitivity analysis of input parameters listed in Table 4 required 323 simulations (based on the maximum frequency of the fourth-order frequency set) with PCGC-2 to obtain the appropriate sensitivity measurements. The complete sensitivity analysis required approximately 50 CPU hours on a Cray 1S. An analysis of this magnitude previously had not been conducted so techniques were developed to perform the analysis. In addition to facilitate conducting the sensitivity analysis on the Cray computers, certain operating procedures were established.

Because parametric variance was identified from both the literature survey and expert experience and because there was no most probable value identified in the range, it was desired to give equal weighting to all parameter values over their range. Thus, the uniform distribution function shown in Eq. 7 was used:

$$f(\alpha_i; N) = \frac{1}{N} \tag{7}$$

where α_i is the parameter and N is the number of simulations conducted in the analysis. In most cases, the error is assumed to have a normal distribution about some mean value. However, in this study a uniform error function was utilized to represent the knowledge or lack thereof concerning the distribution of each parameter over its range. The analysis was

conducted with the parameter ranges and the PDFs discussed previously.

Sensitivity Analysis Results

Results of the sensitivity analysis for each output function considering the different parameters are typically characterized by three basic variables which can conveniently be established from the Fourier coefficients. The Fourier coefficients are obtained by transforming the multidimensional parameter space (nine dimensions in this case) into a one-dimensional search domain. The resulting function is sampled over the appropriate number of simulations (323 in this case) and the output is Fourier analyzed. The one-dimensional output function in "s" can be represented by the Fourier expansion as:

$$u^i(\alpha(s)) = \frac{A_0}{2} + \sum_{j=1}^{n} [A_j^i \cos(js) + B_j^i \sin(js)] \tag{8}$$

$$A_j^i = \frac{1}{\pi} \int_{-\pi}^{\pi} u^i(s) \cos(js) ds$$

$$B_j^i = \frac{1}{\pi} \int_{-\pi}^{\pi} u^i(s) \sin(js) ds$$

The first sensitivity variable is the average functional value which is computed over all model simulations:

$$< u(s) >_s^i = \lim_{T \to \infty} \frac{1}{T} \int_{-T}^{T} u^i(s) ds = \frac{A_0^i}{2} \tag{9}$$

This represents the best calculation from the model considering all possible uncertainties, caused by either experimental error or inherent parameter uncertainty. This can be compared to a base case calculation with PCGC-2 using mean values for the input parameters listed in Table 2.

The second variable is the standard deviation which represents the amount the function deviates from its mean value. This is obtained by Parseval's formula for Fourier series:

$$\sigma_{\text{total}}^i = \left[\sum_{j=1}^{2n-1} \left(A_j^{(i)2} + B_j^{(i)2} \right) + \left(\frac{A_0^{(i)}}{2} \right)^2 \right]^{1/2} \tag{10}$$

where n is the number of simulations. This variable indicates regions where the function deviates greatly due to parametric uncertainty. Large functional deviation in one region can dominate code predictions for other regions of the domain.

The standard deviation does not identify contributions from specific parameters. However, it is possible to define partial variances (third variable) that represent the fraction of the total deviation caused by uncertainty in an individual parameter:

$$S_j^i = \frac{\sigma_j^{(i)2}}{\sigma_{\text{total}}^{(i)2}} \tag{11}$$

Coupled partial variances are also calculated and represent the fraction of total deviation caused by the coupled effect of uncertainty in two parameters:

$$S_{jk}^i = \frac{\sigma_j^{(i)2} + \sigma_k^{(i)2}}{\sigma_{\text{total}}^{(i)2}} \tag{12}$$

This represents variance in the ith output caused by uncertainty in the jth and kth parameters. Thus, partial variances indicate which parameters have the greatest impact on model predictions.

In some cases, not all functional deviation is accounted for by the single or double partial variances. This phenomenon represents higher-order parameter coupling. A sensitivity variable, Deviation-Accounted-For (D_a) was defined to illustrate the high-order coupling between model parameters and model predictions:

$$D_a^i = \frac{\sum_{j=1}^{n} S_j^i + \sum_{j=1}^{n} \sum_{k=1}^{n} S_{jk}^i}{\sigma_{\text{total}}^{(i)2}} \tag{13}$$

This variable illustrates regions where the frequency set (Fourth-order) used in the sensitivity analysis was not capable of elucidating parameter interactions.

Besides the main sensitivity variables, further sensitivity information can be obtained by examining the Fourier sine coefficients. Cukier (1973) shows that this coefficient is directly proportional to the linear sensitivity coefficient $< du_i/d\alpha_j >$ as:

$$B_j^i = < \frac{\partial u_i}{\partial \alpha_j} > + O(\alpha^2) \tag{14}$$

where the second term on the right represents the higher-order nonlinear terms. Examination of the sine coefficients provides an indication of the relationship between individual parameters and specific model output.

Predicted burnout

The average predicted burnout over the entire simulation set is shown in Figure 1a. Also shown is the calculated standard deviation for the predicted burnout. The calculated standard deviation corresponds to a PDF describing probable values of predicted burnout. If this PDF were normal then the standard deviation shown in Figure 1a would account for about 68% of the probable values of predicted burnout. Included in Figure 1a are three calculated PDF's derived from frequency plots of calculated burnout for all simulations. Reactor locations corresponding to the PDF's are representative of the early reactor region (high particle heating rates), the immediate post flame region (fuel-rich zone) and the well mixed region (reactor exit). Deviation in predicted burnout increases from 0–10% in the first region while it reaches a maximum of 15% in the next region after which it decreases to about five percent at the reactor exit. Also included in this plot is a comparison to both the predicted burnout from the base case and the experimentally measured values (Asay, 1982).

Figure 1b shows the parameters which account for over 90% of the functional deviation in mixing cup (radially averaged) burnout along the axial length of the reactor. Uncertainty in the activation energy for the high temperature devolatilization

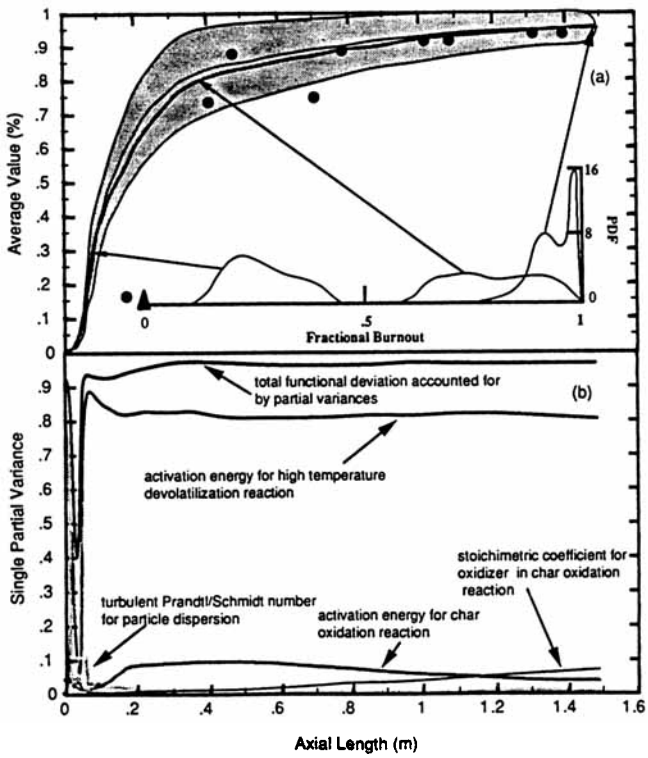

Figure 1. Sensitivity for predicted Mixingcup Burnout.

(a) Comparison of Base case prediction (——) to the average value prediction (——) with associated standard deviation (□). Experimental burnout measurements (Asay, 1982) included for comparison (•); (b) fraction of functional deviation attributed to individual parameters: activation energy for high temperature devolatilization reaction (• • • •), activation energy for char oxidation reaction (—•—), turbulent Prandtl/Schmidt number for particle dispersion (—••—), stoichiometric coefficient for oxidizer in char oxidation reaction (——), total functional deviation accounted for by partial variances (——).

reaction accounts for over 80% of this calculated deviation. Even though this partial variance first becomes important in the second zone of the reactor where devolatilization begins, it dominates the calculated uncertainty in burnout for the remainder of the reactor. This demonstrated sensitivity in the post ignition region of the reactor illustrates the dominant effect that overall volatile yield has on the burnout prediction. Thus, future work should focus on obtaining accurate measures of these parameters with an emphasis on getting accurate predictions of the overall volatile yield.

Both the calculated and the measured values, with the exception of two points, lie well within the calculated deviation for the predicted burnout. The deviation envelope represents a prediction incorporating both the experimental and inherent variance in the rate constants required by the devolatilization submodel. It is apparent that the two equation devolatilization submodel used in PCGC-2 does an admirable job of describing the devolatilization process in the reactor in consideration of the parameter uncertainty. The first data point is outside the deviation, because PCGC-2 predicts the ignition point to be earlier in the reactor than the measured data indicate. Both a fundamental lack of understanding of the devolatilization process (which dominates the location of the ignition point) and the experimental technique used to measure this data near the ignition point may account for this disparity. Uncertainty in the devolatilization submodel parameters produces the greatest error in predicting both the ignition point and the overall carbon conversion in the early regions of the reactor. Thus, uncertainty in the devolatilization parameters may control the prediction of ignition point location and the overall carbon conversion. However, once ignition occurs the particle undergoes rapid heating which leads to further devolatilization (Kobayashi et al., 1977). This process continues until the volatiles have been expelled from the particle. Thus, the particle heating rate controls the amount of devolatilization the particle will experience. If ignition is predicted to occur too early in the reactor, combustion may be limited by the amount of oxidizer available for reaction with the volatiles. This may cause lower particle heating rates which would in turn reduce the overall volatile yield. Thus, accurate prediction of the ignition point could control the predicted volatile yield and the overall carbon conversion. Further sensitivity work may help answer the question of how predicted volatile yield is related to ignition point. Regardless of which controls, accurately predicting both the overall volatile yield and the ignition point are shown to be the dominant factors governing the overall coal burnout prediction. Thus, future development work should focus on these aspects of the submodel. Also, better predictions from the existing devolatilization submodel may be realized by obtaining more accurate kinetic data as related to overall volatile yield.

The second largest partial variance is caused by uncertainty in the activation energy for the char oxidation reaction. The magnitude of this partial variance increases as the partial variance associated with the devolatilization process decreases which shows the initiation of char oxidation. The partial variance corresponding to char oxidation remains the second largest contributor to the overall variance in burnout until the last portion of the reactor. At this point, uncertainty in the stoichiometric coefficient for char oxidation reaction becomes the second largest contributor to the overall uncertainty in predicted burnout. This suggests that the oxidation mechanism becomes important near the reactor exit. Thus, it would be beneficial to carry out a study of the char oxidation mechanism under conditions similar to those which exist in the last portion of the reactor.

The last parameter exhibiting a significant impact on the calculated deviation for predicted burnout is the turbulent Prandtl/Schmidt number. This parameter is associated with turbulent particle dispersion. The partial variance corresponding to this parameter is important very early in the reactor, prior to devolatilization. At present, PCGC-2 models the turbulent particle dispersion process through a Fickian dispersion method. Five different size classifications of particles are used to model the particle-size distribution in this study. The impact that particle-size distribution has on calculations with PCGC-2 has previously been demonstrated (Sowa, 1986). The trajectories of the smaller particles can be influenced by the gas flow more dramatically than the large particles. The swirl component of the inlet gas stream has been shown to increase combustion efficiency via several mechanisms (Sloan and Smoot, 1986). One such mechanism is the effect that the swirl has on helping to mix hot active species with fresh reactants through large turbulent diffusion in recirculation zones near the reactor inlet. Since smaller particles could be entrained in these recir-

culation zones more readily than the large ones, they would become an important factor in stabilization of the flame front through the devolatilization process. This may explain the apparent sensitivity of the turbulent disperion parameter. It also helps to emphasize the impact that particle-size distribution has on overall predictions of coal burnout.

Another insight gained from this analysis is the fact that although devolatilization occurs early in the reactor, it is not limited to that region. Indeed, larger particles continue to devolatilize throughout the remainder of the reactor. The same is true for char oxidation. The smaller particles require less time to heat up, and thus they devolatilize first. The larger particles require more time to heat up, and will thus devolatilize further down the reactor. Therefore, devolatilization and oxidation occur concurrently with the smaller particles burning out first, followed by the larger ones. The fact that the small particles burnout more quickly can also affect the devolatilization mechanism. Enhanced burnout of small particles will increase the gas temperature which will in turn cause the high temperature devolatilization reaction to dominate the low temperature reaction. This also explains the dominant effect of the activation energy for the high temperature reaction in the devolatilization mechanism.

The single partial variances shown in Figure 1b account for more than 80% of the total deviation in burnout. This indicates that there is no significant two-way or higher parameter coupling effects present. The same is indicated by the plot of Deviation-Accounted-For. Thus, the frequency set selected for the second step of the sensitivity study was capable of identifying the important parameter sensitivities.

Predicted NO_x concentration

The predicted average value for NO_x concentration is compared to the predicted NO_x concentration from the base case in Figure 2a. As before, the two compare very well. However, in this instance there appears to be a disparity of about 30 ppm at the maximum average value. This region also exhibits the largest calculated functional deviation (about 200 ppm). This occurs in the oxidation zone (zone 3) at about 0.8 meters down the reactor. At this point, the oxidizer has mixed thoroughly with the fuel and NO_x formation is at a peak. Further down the reactor, NO_x is converted to nitrogen or reacts heterogeneously with char to form some other nitrogen species. Thus, the effects of parameter uncertainty are most important in this region of the reactor.

Figure 2b presents the significant, calculated, partial variances caused by parameter uncertainty. As before, the main effect is caused by uncertainty in the activation energy for the high temperature devolatilization reaction. For the calculated burnout this partial variance was insignificant in the very early portion of the reactor, suddenly increased in importance at the flame front (about 0.1 m down the reactor), and remains dominant thereafter. Conversely, for NO_x, this partial variance is initially dominant at the inlet, decreases dramatically at the flame front (about 0.1 m down the reactor), slowly builds in importance to the region where NO_x formation is at its maximum value (0.8 m down the reactor) and remained dominant to the end of the reactor. The Deviation-Accounted-For follows much the same path as the partial variance for this parameter. There appears to be a large amount of high-order coupling at the flame front, although it is impossible to identify

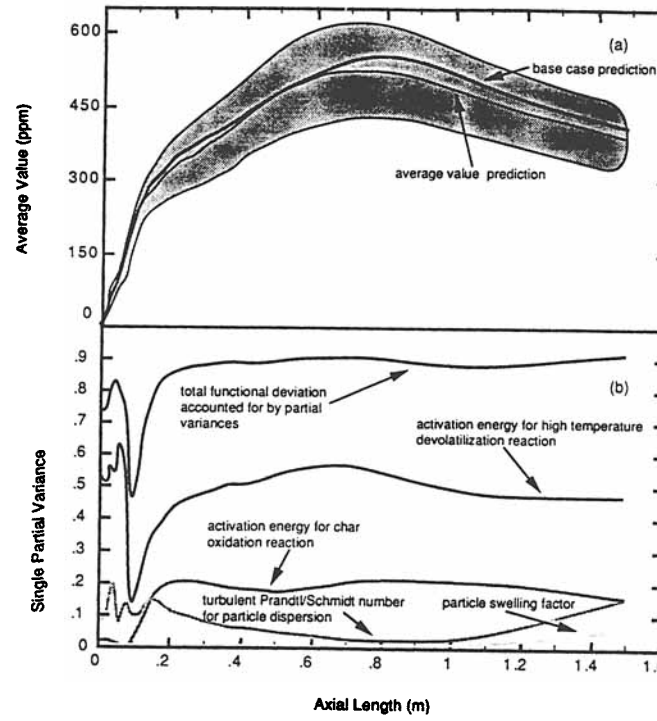

Figure 2. Sensitivity for predicted Mixingcup NO_x concentration.

(*a*) Comparison of Base case prediction (——) to the average value prediction (——) with associated standard deviation (▨); (b) fraction of functional deviation attributed to individual parameters: activation energy for high temperature devolatilization reaction (• • • •), activation energy for char oxidation reaction (—•—), turbulent Prandtl/Schmidt number for particle dispersion (—••—), particle swelling factor (——), total functional deviation accounted for by partial variances (——).

which parameter uncertainties cause this coupling, because of the frequency set used in this analysis. This is not critical though, since the total calculated deviation for NO_x at this point is only 40 ppm compared to more than 200 ppm later on. Also, immediately following the region which indicates high-order coupling, the Deviation-Accounted-For increases to and remains at more than 90% for the rest of the reactor. Thus, the partial variances provide the necessary information on the controlling processes.

Uncertainty in the Prandtl/Schmidt number is the second most important factor early in the reactor and again at the exit of the reactor. This is indicative of the importance of turbulent particle dispersion. Particle dispersion was shown to be important to coal burnout early in the reactor. This was attributed to its effect on flame front formation due to the devolatilization of small particles. It follows that this same process would affect NO_x formation. In this instance, the NO_x formed would be from nitrogen bound in the fuel structure and released during the devolatilization process. Dispersion effects, indicated by the corresponding partial variance near the reactor, may be due to dispersion of char particles resulting in NO_x destruction by char oxidation. This could be quantified by examining a plot of the sine coefficients. If the coefficients are negative, then an increase in this parameter (corresponding to an increase in particle dispersion) would result in a decrease in the predicted NO_x concentration at the reactor exit.

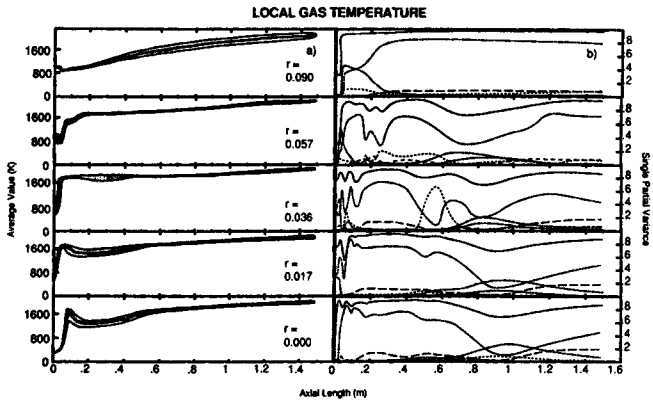

Figure 3. Sensitivity for predicted Local Gas Temperature.

(*a*) Comparison of Base case prediction (——) to the average value prediction (——) with associated standard deviation (▨), (b) fraction of functional deviation attributed to individual parameters: activation energy for high temperature devolatilization reaction (• • • •), activation energy for char oxidation reaction (—•—), turbulent Prandtl/Schmidt number for particle dispersion (—••—), stoichiometric coefficient for oxidizer in char oxidation reaction (——), elemental mass fraction of oxygen in coal (——), stoichiometric coefficient for high temperature devolatilization reaction (——), total functional deviation accounted for by partial variances (——).

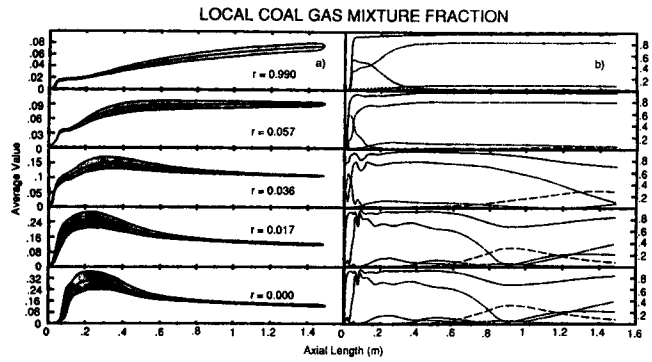

Figure 4. Sensitivity for predicted Local Coal Gas Mixture Fraction.

(a) Comparison of Base case prediction (——) to the average value prediction (——) with associated standard deviation (▨); (b) fraction of functional deviation attributed to individual parameters: activation energy for high temperature devolatilization reaction (• • • •), activation energy for char oxidation reaction (—•—), turbulent Prandtl/Schmidt number for particle dispersion (—••—), stoichiometric coefficient for oxidizer in char oxidation reaction (——), stoichiometric coefficient for high temperature devolatilization reaction (——), total functional deviation accounted for by partial variances (——).

Finally, it is interesting to note the increased effect of uncertainty in the particle swelling parameter at the end of the reactor. This indicates a link between greater char particle surface area and NO_x concentration. It may result from the formation of fuel NO_x by enhancing the release of the remaining nitrogen in the char matrix.

Local gas temperature

The average value of the local gas temperature in the axial direction and at five radial positions of the reactor is shown in Figure 3a. This function is shown in two dimensions to illustrate the multidimensional effects involved in modeling pf combustion. Again, the average value, calculated during the sensitivity analysis, is compared to the base case predictions. This comparison shows no major disparities between the average temperature and the base case temperature. Also, there is relatively very little calculated functional deviation caused by parameter uncertainty. The greatest deviation on the centerline occurs in Zone 1 (flame front) and represents approximately 600 K. This deviation is caused primarily by the change in the predicted ignition point. Again, it illustrates both the difficulty and the importance of predicting this phenomenon. As one moves in the radial direction away from the reactor centerline, the region of greatest deviation shifts. This indicates the two-dimensional nature of the flame. In the first three radial positions, the deviation envelope persists for a short axial distance in the reactor (corresponding to the flame front). The magnitude of the deviation (width of the envelope) becomes smaller until it is almost uniform at the fourth radial point ($r = 0.057$ m). However, at the last radial point ($r = 0.090$ m) the deviation envelope shows significant increase over the last two reactor zones. This indicates the impact parameter error would have on heat flux at the wall. Critical parameters for each radial position can be identified to provide insight into the controlling mechanisms in each reactor region.

Figure 3b presents the significant partial variances for each radial position. As expected, the parameters identified as important to burnout and NO_x concentration show up here. Specifically, the turbulent dispersion, devolatilization, and oxidation parameters (Parameters 1, 3, 5 and 7 from Table 4). However, two new parameters show importance; the stoichiometric coefficient for the high temperature devolatilization reaction (Parameter 4) and the elemental mass fraction of oxygen in the coal particle (Parameter 6). It is interesting to note that these parameters exhibited marginal importance in the screening design. At the first two radial locations (near the centerline) where the volatiles are formed, Parameter 4 accounts for a significant portion of the calculated deviation. Even though the partial variance for this parameter is overshadowed by the partial variance caused by Parameter 3, the variance caused by uncertainty in this parameter further emphasizes the importance of the devolatilization process. Since the devolatilization process occurs at the flame front, it is not surprising that this parameter uncertainty is important near the centerline and less significant near the outer reactor wall. Partial variance caused by uncertainty in Parameter 6 becomes important as one moves from the centerline toward the reactor wall. This indicates the effect that coal rank has on combustion characteristics. According to Singer (1981), the elemental oxygen content of coal is a good guide to coal rank. Thus, the impact of this parameter on predicted gas temperature shows this relationship. A more detailed discussion of the significance of the other partial variances shown in Figure 3b can be found elsewhere (Smith, 1987).

Local coal gas mixture fraction

The average value for the local coal gas mixture fraction as a function of both the axial and radial directions in the reactor are shown in Figure 4a. Again, these values are compared to

those from the base case calculation. Only slight differences between the two values are noticeable. These differences occur in the first reactor zone corresponding to the flame front. Since the coal-gas mixture fraction relates both the mixing and the kinetic processes, sensitivity analysis results for this output function provide insight into the coupling of these important phenomena. This coupling can be seen by noting the large calculated functional deviation near the early regions of the reactor centerline. Here, the amount of coal-gas evolved varies greatly due to the predicted change in flame front location. In later regions of the reactor, there is essentially no deviation in this output function which indicates no relationship to parameter uncertainty. However, as one moves away from the reactor centerline the calculated deviation in the latter regions of the reactor becomes more significant. This deviation is caused by uncertainty in the devolatilization parameters. As with burnout, this shows the effect of parameter uncertainty on predicting the ignition point and overall volatiles yield. The shift in the deviation envelope again illustrates the two-dimensional nature of the flame front. This is further illustrated by examining the partial variances shown in Figure 4b. As before, the dominant effects are attributed to the devolatilization and oxidation parameters. However, uncertainty in the stoichiometric coefficient for the high temperature devolatilization reaction appears significant near the centerline and uncertainty in the turbulent dispersion parameter appears important near the reactor wall. These apparent significant effects occur in regions where the total deviation envelope is relatively small. Thus, these partial variances have only a small impact on the overall predictions. The observed deviation in the coal-gas mixture fraction near the wall most likely is caused by recirculating gas coming from farther down the reactor. This fact may be the reason for the apparent impact of the turbulent dispersion parameter on the coal-gas mixture fraction near the outer wall (as discussed earlier).

Evalidation of the two-step analysis approach

Having performed this detailed two-step sensitivity analysis of PCGC-2, two questions regarding the study require consideration:

1. Are the results of the study biased by doing the linear study first and then only considering parameters identified in the linear analysis during the nonlinear analysis?
2. What extra value (additional information) is there in doing the second nonlinear step of the analysis?

These questions can be addressed by reviewing the methodology and results of this study.

The first question is concerned with the loss of sensitivity information caused by only considering parameters in the second nonlinear part of the study that were identified during the initial screening design. The first step of the study, a linear screening design, is meant to identify the main parameter interactions. This assumes that primary (one-way) effects cause the largest variance in the output functions and that these effects can be accurately identified by a linear screening design. Also, using an initial screening design to identify primary effects can save time.

The alternative would be to perform a nonlinear analysis of the entire parameter set (19 in this case). As indicated earlier, to obtain nonbiased results from a nonlinear analysis this would require approximately 6,000 simulations (see Eq. 6). This level of work clearly would be unreasonable, and we require a way to reduce the number of simulations required to analyze a complex model with large numbers of input parameters. The assumption that single parameter effects have the largest impact on functional variance can be tested by examining the results from the second, nonlinear, step of the analysis.

Examining the one-way parameter interactions shown in Figures 1-4 shows that primary effects (partial variance caused by error in parameter 3) are much larger than any secondary effects (partial variance caused by error in parameter 3 interacting with the uncertainty in any other parameter). Another indication of the validity of this assumption is given by the sensitivity analysis variable, D_a. The primary effects shown in Figures 1-4 account for more than 80% of the total functional variance in every case. These two facts verify the ability of the two-step methodology used during this study to identify key parameter effects during the screening design without comprising the results of the overall sensitivity analysis.

The second question that requires attention is concerned with the added benefit of doing the second, nonlinear analysis of the study. As pointed out earlier, the model examined during this study is composed of several nonlinear, coupled partial differential equations and many auxiliary equations required to describe the complex processes involved in pulverized-coal combustion. Thus, to fully examine the impact that parameter uncertainty has on model predictions it is necessary to perform a nonlinear analysis. Although no significant coupled partial variances (secondary effects) were identified in this particular case study, there was no way of insuring this beforehand. And, this result does not guarantee that secondary effects will not be important in other studies of highly nonlinear systems. Thus, without performing the second nonlinear analysis step of the present methodology the results of this study would be questionable.

This study demonstrates that future modeling efforts should be focused on a better definition of the parameters governing particle devolatilization/oxidation mechanisms. This effort should focus on providing better predictions of the ignition point and overall volatile yields. An integral part of that work must include efforts to quantify the physical parameters describing the turbulent kinetic, mass-transfer, and heat-transfer processes involved in the devolatilization/oxidation mechanisms. Additional work must also focus on developing a better definition of the turbulent particle dispersion mechanism. These conclusions are not unique to this discussion and work has been underway to obtain a better understanding of these mechanisms. The results presented here do conclusively demonstrate the need to incorporate the best knowledge (from the laboratory) concerning critical mechanisms into better numerical submodels which make up comprehensive computer models describing complex phenomena such as pf combustion.

Additional sensitivity analysis work should be conducted to examine the impact that particle size has on turbulent dispersion and ignition point. The relationship between ignition point and volatile yield should also be investigated to determine the controlling process according to the two equation devolatilization submodel presently used in PCGC-2.

While the results obtained in the sensitivity analysis are case-specific, they do focus attention on the critical submodels which appear to dominate the predictions. These results pro-

vide direction to future submodel development as well as experimental efforts to obtain accurate values of the physical parameters required by these submodels. This work also illustrates the role of sensitivity analysis as an engineering tool to be used to gain a deeper understanding of the physical process being modeled. In addition, the techniques used to perform this study may aid in future sensitivity studies of large computer models describing physical systems in a realistic fashion.

Acknowledgments

This work was supported by funding from a consortium of industrial and governmental agencies administered through Brigham Young University. The illustrations were prepared by Linda Ward. Editorial assistance was also provided by Dr. L. D. Smoot.

Notation

A = cosine coefficient in Fourier expansion
B = sine coefficient in Fourier expansion
D_a = functional deviation accounted for by partial variances from FAST
$f(\alpha_i)$ = probability density function representing the ith parameter uncertainty
L = general mathematical operator in Eq. 1
n = number of parameters examined in sensitivity analysis
N = number of simulations conducted in sensitivity analysis
$P(\alpha_i)$ = probability for ith parameter
r = radial dimension in cylindrical coordinate system
$\mathbf{S}$ = general forcing function or source term in Eq. 1
S_j = single partial variance defined by Eq. 11
S_{jk} = two-way partial variance defined by Eq. 12
u = axial velocity component
$u(s)$ = one-dimensional search function used in FAST to approximate n-dimensional parameter space
$u(x, \alpha)$ = vector or model outputs as functions of the independent variables (x) and model parameters (α)
v = radial velocity component
x = axial dimension in cylindrical coordinate system

Greek letters

α = represents a general model parameter
Γ_ϕ = diffusion coefficient for transport property ϕ
ρ = fluid density (mass/volume)
σ^2 = total variance of function
ϕ = transport property

Literature Cited

Asay, B. W., "Effects of Coal Type and Moisture Content on Burnout and Nitrogenous Pollutant Formation," PhD Dissertation, Brigham Young University, Provo, UT (1982).

Atherton, R. W., R. B. Schainker, and E. R. Ducot, "On the Statistical Sensitivity Analysis of Models for Chemical Kinetics," *AIChE J.*, **21**(3), 441 (1975).

Boni, A. A., and R. C. Penner, "Sensitivity Analysis of a Mechanism for Methane Oxidation Kinetics," *Comb. Sci. Tech.*, **15**, 99 (1977).

Caracotsios, M., and W. E. Stewart, "Sensitivity Analysis of Initial Value Problems with Mixed ODEs and Algebraic Equations," *Comput. Chem. Eng.*, **9**, 231 (1985).

Coffee, T. P., and J. M. Heimerl, "Sensitivity Analysis for Premixed, Laminar Steady State Flames," *Comb. and Flame*, **50**, 323 (1983).

Cukier, R. I., C. M. Fortuin, and K. E. Shuler, "Study of the Sensitivity of Coupled Reaction Systems to Uncertainties in Rate Coefficients. I. Theory," *J. Chem. Phys.*, **59**, 3873 (1973).

Cukier, R. I., J. H. Schaibly, and K. E. Shuler, "Study of the Sensitivity of Coupled Reaction Systems to Uncertainties in Rate Coefficients. I. Analysis of the Approximations," *J. Chem. Phys.*, **63**, 1140 (1975).

Cukier, R. I., H. B., Levine, and K. E., Shuler, "Nonlinear Sensitivity Analysis of Multiparameter Model System," *J. Comp. Phys.*, **26**, 1 (1978).

Daniel, C., *Applications of Statistics to Industrial Experimentation*, Wiley, New York (1976).

Dickinson, R. P., and R. J. Gelinas, "Sensitivity Analysis of Ordinary Differential Equations—A Direct Method," *J. Comp. Phys.*, **21**, 123 (1976).

Dougherty, E. P., and H. Rabitz, "A Computational Algorithm for the Green's Function Method of Sensitivity Analysis in Chemical Kinetics," *Int. J. Chem. Kinet.*, **11**, 1237 (1979).

Dunker, A. M., "Efficient Calculation of Sensitivity Coefficients for Complex Atmospheric Models," *Atmos. Env.*, **15**(7) 1155 (1981).

Falls, A. H., G. J. McRae, and J. H. Seinfeld, "Sensitivity and Uncertainty of Reaction Mechanisms for Photochemical Air Pollution," *Int. J. Chem. Kinet.*, **11**, 1137 (1979).

Fletcher, T. H., "A Two-Dimensional Model for Coal Gasification and Combustion," PhD Dissertation, Brigham Young University, Provo, UT (1983).

Frank, P. M., *Introduction to System Sensitivity Theory*, Academic Press, New York (1978).

Hwang, J., E. P. Dougherty, S. Rabitz, and H. Rabitz, "The Green's Function Method of Sensitivity Analysis in Chemical Kinetics," *J. Chem. Phys.*, **69**(11), 5180 (1978).

Hwang, J. T., "Sensitivity Analysis in Chemical Kinetics by the Method of Polynomial Approximation," *Int. J. Chem. Kinet.*, **15**, 395 (1983).

Hill, S. C., "Modeling of Nitrogen Pollutants in Turbulent Pulverized-Coal Flames," PhD Dissertation, Brigham Young University, Provo, UT (1983).

Jerri, A. J., "The Shannon Sampling Theorem—Its Various Extensions and Applications: A Tutorial Review," *Proc. of the IEEE*, 65 (1965).

Kobayashi, H., J. B. Howard, and A. F. Sarofim, "Coal Devolatilization at High Temperatures," *16th Symposium (International) on Combustion*, The Combustion Institute, Pittsburgh, PA, 411 (1977).

Koda, M., G. McRae, and J. H. Seinfeld, "Automatic Sensitivity Analysis of Kinetic Mechanisms," *Int. J. Chem. Kinet.*, **11**, 427 (1979).

Kramer, M. A., J. M. Calo, and H. Rabitz, "An Improved Computational Method for Sensitivity Analysis: Green's Function Method with 'AIM'," *App. Math. Modelling*, **5**, 432 (1981).

Kuntz, P. J., G. F. Mitchell, and J. Ginsburg, "Fourier Analysis of Steady-State Reaction Schemes for Interstellar Molecules," *Astrophys. J.*, **209**, 116 (1976).

Pierce, T. H., "Theory and Application of Sensitivity Analysis to Enzyme Kinetics," PhD Dissertation, Michigan State University, East Lansing, MI (1981).

Pierce, T. H., and Cukier, R. I., "Global Nonlinear Sensitivity Analysis Using Walsh Functions," *J. Comp. Phys.*, **41**, 427 (1981).

Plackett, R. L. and J. P. Burman, "The Design of Optimum Multifactorial Experiments," *Biometrika*, **33**, 305 (1946).

Rabitz, H., "Chemical Sensitivity Analysis Theory with Applications to Molecular Dynamics and Kinetics," *Comput. Chemistry*, **5**, 167 (1981).

Rabitz, H., M. Kramer, and D. Dacol, "Sensitivity Analysis in Chemical Kinetics," *Ann. Rev. Phys. Chem.*, **34**, 419 (1983).

Rasband, M., "A Combined Analysis of the Data Book and PCGC-2," MS Thesis, Brigham Young University, Provo, UT, in progress (1987).

Reuven, Y., M. D. Smooke, and H. Rabitz, "Sensitivity Analysis of Boundary Value Problems: Application to Nonlinear Reaction-Diffusion Systems," *J. Comp. Phys.*, **64**, 27 (1986).

Schailby, J. H., and K. E. Schuler, "Study of the Sensitivity of Coupled Reaction Systems to Uncertainties in Rate Coefficients. II. Application," *J. Chem. Phys.*, **59**, 3879 (1973).

Singer, J. G., ed., *Combustion, Fossil Power Systems*, Combustion Engineering, Inc., Windsor, CT (1981).

Sloan, D. G., P. J. Smith, and L. D. Smoot, "Modeling of Swirl in Turbulent Flow Systems," *Progr. Energy Combust. Sci.*, **12**, 163 (1986).

Smith, J. D., "Prediction of the Effects of Coal Quality on Utility Furnace Performance," MS Thesis, Brigham Young University, Provo, UT (1984).

Smith, J. D., "Foundations of a Three-Dimensional Model for Predicting Coal Combustion Characteristics in Industrial Power Generation Plants," PhD Dissertation in preparation, Brigham Young University, Provo, UT (1987).
Smith, R. D., "The Trace Element Chemistry of Coal during Combustion and the Emissions from Coal-Fired Plants," *Progr. Energy Combust. Sci.*, **6**, 201 (1980).
Smith, P. J., T. H. Fletcher, and L. D. Smoot, "Model for Pulverized Coal-Fired Reactors," *18th Symposium (International) on Combustion*, The Combustion Institute, Pittsburgh, PA, 1285 (1981).
Smith, P. J., and L. D. Smoot, *Detailed Model for Practical Pulverized Coal Furnaces and Gasifiers*, Quarterly Technical Progress Report No. 6 (Feb., 1987).
Smoot, L. D., and D. T. Pratt, eds., *Pulverized Coal Combustion and Gasification*, Plenum Publishing Corp., New York (1979).
Smoot, L. D., and P. J. Smith, *Coal Combustion and Gasification*, Plenum Press, New York (1985).
Smooke, M. D., Y. Reuven, H. Rabitz, and F. L. Dryer, "Application of Sensitivity Analysis to Premixed Hydrogen-Air Flames," Report ME-104-86, Yale University, New Haven, CT (1986).
Sowa, W., "Effect of Particle Size Distribution on the Simulation of Pulverized Wall Combustion," personal communication, Brigham Young University, Provo, UT (1986).
Tilden, J. W., V. Constanza, G. J. McRae, and J. H. Seinfeld, "Sensitivity Analysis of Chemical Reacting Systems," in *Modeling of Chemical Reacting Systems*, K. H. Ebert, P. Deuflhard, and W. Jager, eds., pp. 69–91, Springer-Verlag, Berlin (1981).
Tomovic, R., and M. Vokobratovic, *General Sensitivity Theory*, Elsevier, New York (1972).

Manuscript received Sept. 26, 1991, and revision received Mar. 23, 1993.